

Graphic Evidence for Non-Abelian Flux Tubes

D. G. Caldi

Department of Physics, University of Connecticut, Storrs, Connecticut 06268

and

T. Sterling

Department of Physics, University of Michigan, Ann Arbor, Michigan 48109

(Received 25 March 1988)

From Monte Carlo calculations of plaquette-Wilson-loop correlations for three-dimensional SU(2) lattice gauge theory, we give unambiguous graphic demonstrations of the formation of non-Abelian chromoelectric flux tubes with constant energy density in the region between a pair of static $q\bar{q}$ sources.

PACS numbers: 11.15.Ha, 12.38.Gc

The formation of narrow tubes of chromoelectric flux is the hallmark of a theory which is supposed to confine objects with color charge, as QCD is all but proven to do. It would be encouraging, as well as useful for more detailed investigations, to demonstrate the existence and formation of actual chromoelectric flux tubes. We have undertaken a laborious computational study of a non-Abelian lattice gauge theory to demonstrate graphically chromoelectric flux tubes and to ascertain some of their properties, such as thickness and the directly associated string tension (the energy/length in the flux string). Since we were interested in as convincing a demonstration as possible, which meant using Wilson loops large enough to see the inside rather than just edge effects, we have in this study been forced by already heavy computer demands to limit ourselves to three-dimensional (3D) SU(2) lattice gauge theory (LGT). Although it is true that while our study was underway, others¹⁻³ have attempted to look at four-dimensional (4D) LGT, we feel that the small size of the Wilson loops they considered produced only suggestive, although indeed very enticing, results.

Three-dimensional non-Abelian gauge theory is of interest not just as a nontrivial model for the more realistic four-dimensional theory, but also because in the high-temperature limit⁴ 3D QCD is the effective theory of 4D QCD. The 3D theory has been investigated both in the continuum⁴ and on the lattice.⁵ Like its 4D counterpart, the lattice theory is believed to confine for all values of the bare lattice coupling g , and confinement is presumed to persist in the continuum limit. However, because the coupling g^2 has dimensions of L^{-1} and the theory is superrenormalizable, there is not sharp transition from strong to weak coupling, unlike in the 4D case. Hence the string tension falls off much more slowly with decreasing g (power rather than exponential falloff), and so it should be much easier to extract results valid in the continuum limit from the lattice. Indeed, standard Monte Carlo studies of the string tension σ for 3D

SU(2) LGT have been done,⁵ with general agreement about the behavior of σ although with some dispute about the details. It should be noted that because we are in three dimensions, the perturbative Coulomb potential $V(R)$ between a quark and antiquark has a logarithmic behavior, $V(R) \propto \ln R$. However, this is not what is meant by confinement. We mean, instead, the nonperturbative linear potential, $V(R) \propto R$, which results from an area-term falloff of the Wilson loop.

The continuum version for a three-dimensional non-Abelian pure gauge theory (what is often called 3D QCD) is defined by the standard action for the gauge fields $A_\mu^a(x)$,

$$S = \frac{1}{4} \int d^3x F_{\mu\nu}^a F_a^{\mu\nu}, \quad (1)$$

with

$$F_{\mu\nu}^2 = \partial_\mu A_\nu^a - \partial_\nu A_\mu^a + g f^{abc} A_\mu^b A_\nu^c. \quad (2)$$

In our case the f^{abc} 's are the structure constants for the group $G = \text{SU}(2)$.

Regulating the theory by means of cubic, Euclidean lattice with spacing a , we define the usual Wilson action in terms of the link variables $U_{n,\mu} \in G$, where n labels the sites and μ the three directions:

$$S_W = 1 - \frac{1}{2} \sum_{n,\mu,\nu} \text{Tr}(U_{n,\mu} U_{n+\mu,\nu} U_{n+\mu+\nu,-\mu} U_{n+\nu,-\nu}). \quad (3)$$

The partition function is then

$$Z = \prod_{n,\mu} dU_{n,\mu} \exp(-\beta S_W), \quad (4)$$

where $\beta = 4/g^2 a$. In the naive continuum limit $a \rightarrow 0$, since we can use the exponential map between group and Lie-algebra elements,

$$U = \exp(iga A_\mu^b \tau^b), \quad (5)$$

We have $S_W \rightarrow S$.

The energy density $\mathcal{E}(\mathbf{x})$ of a gluon field in the presence of a static $q\bar{q}$ pair relative to the ground state without quarks is given by

$$\mathcal{E}(\mathbf{x}) = \langle q\bar{q} | \frac{1}{2} [\mathbf{E}_a^2(\mathbf{x}) + \mathbf{B}_a^2(\mathbf{x})] | q\bar{q} \rangle - \langle 0 | \frac{1}{2} [\mathbf{E}_a^2(\mathbf{x}) + \mathbf{B}_a^2(\mathbf{x})] | 0 \rangle. \quad (6)$$

It should be noted that in (2+1) dimensions, the magnetic field is a scalar. Knowing $\mathcal{E}(\mathbf{x})$, we can obtain directly the string tension by integrating over what would have been the area per unit length in three spatial dimensions, but what here becomes just the line per unit length perpendicular to the string:

$$\int \mathcal{E} dl = [\text{eng}/l] = \sigma. \quad (7)$$

In order to measure the energy densities, we have to be able to put a static $q\bar{q}$ pair in our lattice system in a gauge-invariant way. Unfortunately, the approach adopted by Sterling and Greensite⁶ for the Abelian theory, namely using the so-called polymer formulation combined with individual Wilson lines for the quark and antiquark, does not work in the non-Abelian case since the resulting action becomes complex and hence unsuitable for standard Monte Carlo simulations. Hence, we have been forced to use the more laborious method of putting a Wilson loop in the lattice in order to have a gauge-invariant, static $q\bar{q}$ source. So we have really measured chromoelectric flux surfaces or volumes, i.e., what the tubes sweep out in time.

To measure the energy densities we make use of the fact that the plaquette (P) measures the internal energy. So we pick out one direction arbitrarily as Euclidean time, and measure the plaquette-Wilson-loop correlations, subtracting off the corresponding plaquette energies in the absence of the Wilson loop W :

$$\mathcal{E}_E(\mathbf{x}) = \langle P_{0i}(\mathbf{x})W \rangle / \langle W \rangle, \quad (8)$$

$$\mathcal{E}_b(\mathbf{x}) = \langle P_{12}(\mathbf{x})W \rangle / \langle W \rangle, \quad (9)$$

$$\mathcal{E}_E^0(\mathbf{x}) = \langle P_{0i} \rangle, \quad (10)$$

$$\mathcal{E}_B^0(\mathbf{x}) = \langle P_{12} \rangle. \quad (11)$$

These quantities correspond to the color electromagnetic energy densities in the weak-coupling limit. Then with

$$\mathcal{E}_E = \mathcal{E}_{E_1} + \mathcal{E}_{E_2}, \quad (12)$$

the total energy density for the 3D Euclidean lattice theory is

$$\mathcal{E}(\mathbf{x}) = [\mathcal{E}_E(\mathbf{x}) - \mathcal{E}_B(\mathbf{x})] - [\mathcal{E}_E^0(\mathbf{x}) - \mathcal{E}_B^0(\mathbf{x})]. \quad (13)$$

Note that the change of sign compared to (6) is the result of the Wick rotation to Euclidean space.

We would like to do our measurements as deep in the weak-coupling regime as possible in order to be close to the continuum limit. But there is another reason for our going to large β . In order to measure the chromoelectric flux between the quark-antiquark sources on the Wilson loop, we want to be able to see what is happening inside

the loop and not just measure the energy where the charges are situated. Hence, we must make the loops large enough to have the central region of the loop well isolated from the edges. It is unfortunate fact that large Wilson loops do not become observable until weak coupling because of their exponential suppression. Because of the resulting small signal, as well as from general requirements, we have performed all of our measurements with rather high statistics.

The details of the computations will be published elsewhere.⁷ Suffice it to say here that we worked with a 16^3 periodic lattice and employed the 120-parameter icosahedral finite subgroup of $SU(2)$ in a Metropolis algorithm with multiple hits. We did our plaquette-loop correlation measurements only on square Wilson loops of six 6×6 and 8×8 for $\beta=8$, and 7×7 and 8×8 for $\beta=7$. Each 100 measurements were based on approximately 2500 iterations and we were especially careful to eliminate autocorrelations.⁷ The total number of measurements as well as the average value measured for each Wilson loop are listed in Table I.

Since our main goal was a graphic demonstration of non-Abelian chromoelectric flux tubes, our main results are the type of three-dimensional graph presented in Fig. 1 which is for the 7×7 loop at $\beta=7$. We are plotting the chromoelectric energy density $\mathcal{E}_{E_1}(\mathbf{x})$, Eq. (8), as measured by plaquette-loop correlations for plaquettes parallel to the plane of the Wilson loop, which by definition lies in the 01 plane.⁸ We see in all cases a large, sharp rise in the electric energy where the loop is located and then, more significantly, the flux stays well above background in the middle of the loop. This dramatic signal of confinement is present even in the most recalcitrant example, namely the 8×8 loop for $\beta=7$, where the poor signal-to-noise ratio required 15000 measurements to achieve a picture like Fig. 1.

To make clearer what is happening inside the loop, we have devised plots which average the data for plaquettes in a similar environment due to the symmetry of the loop. Thus as shown in Fig. 2, which is for the 8×8 case, the four inside densities are averaged together and la-

TABLE I. Number of measurements and $\langle W \rangle$.

β	Loop	Measurements	$\langle W \rangle$
8.0	6×6	800	0.0924 ± 0.0011
8.0	8×8	5000	0.0233 ± 0.0011
7.0	7×7	10000	0.0191 ± 0.0010
7.0	8×8	15000	0.00734 ± 0.00076

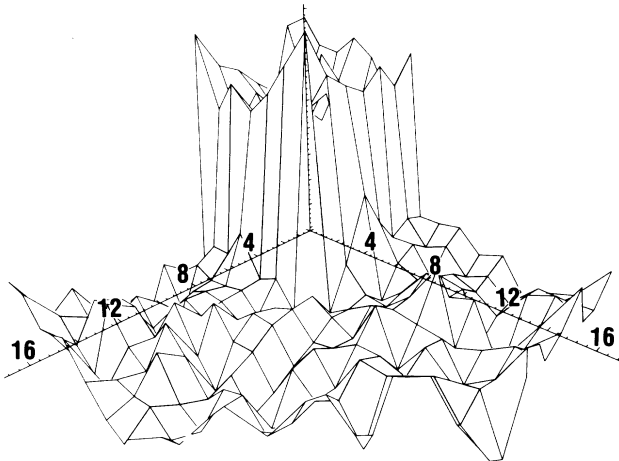


FIG. 1. Chromoelectric energy density parallel to 7×7 loop at $\beta=7.0$. The units are arbitrarily scaled and have only relative significance.

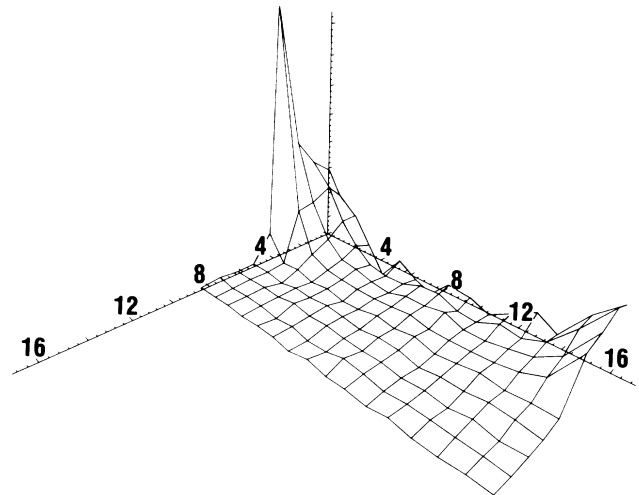


FIG. 3. Averaged energy density for 7×7 loop at $\beta=7.0$. The units are arbitrarily scaled and have only relative significance.

beled 1. Then the densities for the next concentric square "ring" are averaged and called 2, and so forth. Note that because of the periodicity of the lattice, this procedure is exhausted at label 8. We repeat the averaging for each plane parallel to the loop and label the planes 1 through 16, with 1 being the plane of the loop. An example of such a plot, again for the 7×7 loop, is given in Fig. 3. It is quite clear that the chromoelectric flux has become essentially constant and is considerably above background in the region between the $q\bar{q}$ sources, as we expect for a linearly rising potential. To bring this

point into sharper focus, we have plotted the average densities just in the plane of the loop in Fig. 4. The essential constancy of the chromoelectric energy density inside the loop is quite striking in the $\beta=7$ data, with perhaps the suggestion of some Coulomb admixture in the $\beta=8, 8 \times 8$ data. It is also clear that smaller loops could not provide very definitive results.

We also remark that the plots like Fig. 3 give us an indication of the thickness of the flux tubes or strings. It appears to be between 3 and 5 lattice units depending on the size of the loop and β . The significance of this thickening of the string will be discussed elsewhere.⁷

We have also calculated⁷ the string tension directly

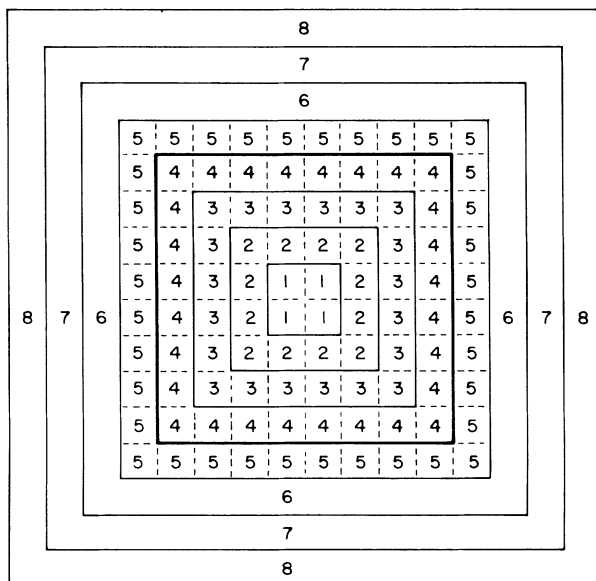


FIG. 2. Method of averaging and labeling convention for energy density in a plane parallel to an 8×8 loop.

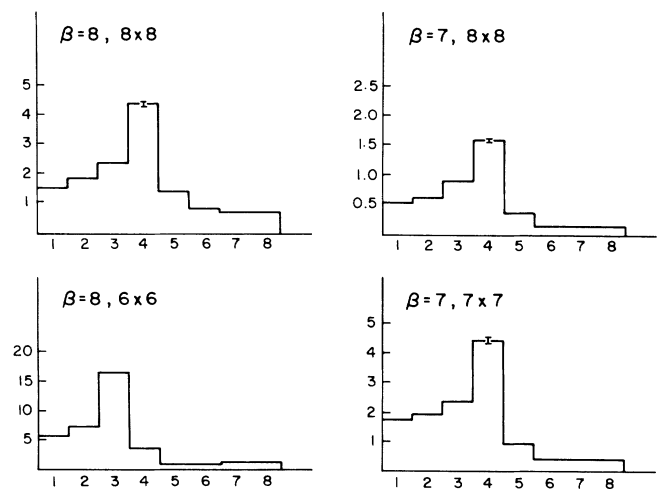


FIG. 4. Averaged energy density in the plane of the loop for the four cases studied. Errors are smaller than the width of the line except where indicated. The units are arbitrarily scaled and have only relative significance.

using Eq. (7). Unfortunately, to use this method and not get large errors, because of the delicate subtraction of the no-source energy density \mathcal{E}^0 , e.g., Eq. (13), one needs to know the expectation value of the Wilson loop to much higher precision than is feasible. So it is not yet clear if there is a significant difference between the directly determined string tensions and those obtained by fitting, as was seen in the Abelian case.

In conclusion, we have presented for the first time unambiguous graphic demonstrations that chromoelectric flux really is confined to narrow regions of space for non-Abelian gauge theory, thus confirming a host of predictions and the suggestive evidence of other studies.

We are grateful for computer time on various Cray supercomputers at the National Magnetic Fusion Energy Computing Center of Lawrence Livermore Laboratory provided by grants of time from the U.S. Department of Energy. One of us (D.G.C.) is a Department of Energy Outstanding Junior Investigator, whose work is supported in part by funds provided by the U.S. Department of

Energy under Contract No. De-AC02-79ER10336. The work of one of us (T.S.) is supported in part by the U.S. Department of Energy.

¹M. Fukugita and I. Niuya, Phys. Lett. **132B**, 374 (1983).

²J. Flower and S. Otto, Phys. Lett. **160B**, 128 (1985).

³J. Wosiek and R. W. Haymaker, Phys. Rev. D **36**, 3297 (1987).

⁴See, e.g., T. Appelquist and R. D. Pisarski, Phys. Rev. D **23**, 2305 (1981).

⁵E. D'Hoker, Nucl. Phys. **B180 [FS2]**, 341 (1981); J. Ambjørn, A. J. G. Hey, and S. Otto, Nucl. Phys. **B210 [FS6]**, 347 (1982); J. Ambjørn, P. Olesen, and C. Petersen, Nucl. Phys. **B240 [FS12]**, 533 (1984).

⁶T. Sterling and J. Greensite, Nucl. Phys. **B220**, 327 (1983).

⁷D. G. Caldi and T. Sterling, to be published.

⁸Similar plots for the other cases studied and plots for the perpendicular electric energy density and the magnetic energy density are presented and discussed in Ref. 7.